Descending from infinity: Convergence of tailed distributions

Christian Van den Broeck
Hasselt University, B-3500 Hasselt, Belgium

Upendra Harbola
Inorganic and Physical Chemistry, Indian Institute of Science, Bangalore 560012, India

Raul Toral
IFISC (Instituto de Física Interdisciplinar y Sistemas Complejos), Universitat de les Illes Balears-CSIC, Palma de Mallorca 07122, Spain

Katja Lindenberg
Department of Chemistry and Biochemistry and BioCircuits Institute, University of California San Diego, La Jolla, California 92093-0340, USA
(Received 6 August 2014; published 15 January 2015)

We investigate the relaxation of long-tailed distributions under stochastic dynamics that do not support such tails. Linear relaxation is found to be a borderline case in which long tails are exponentially suppressed in time but not eliminated. Relaxation stronger than linear suppresses long tails immediately, but may lead to strong transient peaks in the probability distribution. We also find that a δ-function initial distribution under stronger than linear decay displays not one but two different regimes of diffusive spreading.

DOI: 10.1103/PhysRevE.91.012128 PACS number(s): 05.40.−a, 05.20.−y, 02.50.Ey

I. INTRODUCTION

Probability distributions with long tails or diverging moments have fascinated both scientists and nonscientists over many decades because of the unanticipated and even strange behavior that they frequently imply in a large variety of problems ranging from physics, biology, and engineering, to economic and other societal scenarios. Recently, stochastic processes giving rise to such long-tailed distributions have received a great deal of attention because modern technologies have made associated measurements ever more feasible [1]. Our specific purpose in this paper is to investigate how distributions that initially have long or fat tails evolve under stochastic dynamics that do not support such tails.

In view of its wide applicability, we note with some surprise the fact that this problem as described by a Langevin equation with additive white noise seems largely absent in the literature. As we will see, traditional (overdamped) linear Langevin dynamics turn out to be a very interesting borderline case, exhibiting sustained long tails which, however, decay exponentially in time. Langevin equation dynamics with decay rates stronger than linear instantly destroy fat tails, but these may instantly show up as transient maxima in the probability distribution as it relaxes to its steady-state form. While we have not found a discussion of these dynamics, we note that the literature is replete with nonlinear Langevin equation descriptions [2]. Examples of specific stochastic systems and behaviors described by nonlinear Langevin equations include fluid relaxation [3], nonlinear wave interactions [4], the nonlinear dielectric relaxation of asymmetric top molecules [5], the theory of nonlinear elasticity [6], saturation in dilute solutions [7], Brownian motion in a tilted potential [8], diffusion with velocity-dependent friction [9], and diodes as thermal engines [10]. As a more abstract mathematical problem, nonlinear Langevin equations have been discussed in normal form analysis in the presence of noise [11], the effect of the noise on sweeping through a bifurcation [12] or crossing an imperfect bifurcation [13], the connection with intermittency [14], the excitation of pseudoregular oscillations induced by noise [15], and the approach to equilibrium in a logarithmic potential [16].

Indeed, entire books and extensive articles have been written addressing the problem of noise in nonlinear dynamical systems, including Coffey's broad coverage of the Langevin equation in physics, chemistry, and electrical engineering [8], the volumes edited by Moss and McClintock on noise in nonlinear dynamical systems [17], and Rzoska and Zhelezny's collection on nonlinear dielectric phenomena in complex liquids [18]. As a far-reaching continuing topic of interest we mention the broad arena of Brownian motors, many models of which are based on nonlinear Langevin equations, cf. the review in Ref. [19]. And finally, we end this list of applications and coverage of nonlinear Langevin equations with the quintessential and perhaps most broadly known problem of Kramers' escape over a potential barrier [20]. All of these problems are affected by the behavior discussed herein on initial conditions with fat tails.

Before launching into an analysis of our fat-initial-tail problem, we note that in the process of relaxing to the steady state we observe another interesting phenomenon that we have not seen discussed. While the usual expectation is that a δ-function initial condition spreads diffusively until it reaches the steady-state form, this happens only in the case of linear dynamics. When the decay rates are stronger than linear, the relaxation to the steady state displays not one but two distinctly separate regimes of diffusive spreading. We examine the origin of this phenomenon and determine the time at which the relaxation process transitions from one to the other.

To arrive at an understanding of the stochastic dynamics, we begin by analyzing the deterministic dynamics of equations of the form $dx/dt = -\gamma x^{\alpha}$ where $\alpha \geqslant 1$. These dynamics, simple as they are, already exhibit the underlying reasons for the unusual stochastic relaxation. We dedicate Sec. II to this analysis for δ-function initial conditions. These results in turn already reflect the interesting behavior found, still with deterministic dynamics, when the initial condition is distributed. This is covered in Sec. III. In the next two sections we add noise to the system, first in the case of linear relaxation in Sec. IV and then for nonlinear relaxation in Sec. V. We conclude with a short summary in the final section. Some mathematical details are relegated to an Appendix.

II. DETERMINISTIC DYNAMICS

A direct integration of the deterministic evolution equation

$$\frac{dx}{dt} = -\gamma x^{\alpha} \tag{1}$$

leads to $x_t^{1-\alpha} = x_0^{1-\alpha} + (\alpha - 1)\gamma t$, or

$$x_t = \frac{x_0}{\left[1 + (\alpha - 1)x_0^{\alpha-1}\gamma t\right]^{\frac{1}{\alpha-1}}}, \tag{2}$$

where x_0 is the initial condition. In the limit $\alpha \to 1$, Eq. (2) reduces to the familiar exponential solution $x_t = x_0 e^{-\gamma t}$. Without loss of generality we set $\gamma = 1$, since this can always be achieved by rescaling the time variable, $t \to \gamma t$. The solution (2) is a well-defined real function for all values of x regardless of the value of α if the initial condition is positive, $x_0 > 0$. If the initial condition is negative, $x_0 < 0$, then the requirement that $x^{\alpha-1}$ be a well-defined real function for all values of x is satisfied, for instance, if α is an integer. Alternatively, we could replace Eq. (1) with $\dot{x} = -\gamma x|x|^{\alpha-1}$ to remove the requirement that α must be an integer. All subsequent formulas are then valid for all x if we replace $x^{\alpha-1}$ by $|x|^{\alpha-1}$.

We point out the following peculiar features of the above solution, see for example Ref. [21]. For $\alpha > 1$, the decay rate x^{α} becomes very strong for x large, so much so that infinity moves down to a finite value x_t^+ at any finite time t. More precisely, the entire positive x axis $x \in [0,\infty)$ is, for any finite time t, mapped by the dynamics into a finite interval $[0,x_t^+)$, with

$$x_t^+ = \frac{1}{[(\alpha - 1)t]^{\frac{1}{\alpha-1}}}. \tag{3}$$

This value is obtained by considering the limit $x_0 \to \infty$ in Eq. (2). Note that one can rewrite Eq. (2) in the following more compact form:

$$\frac{x_t}{x_0} = [1 + (x_t^+/x_0)^{1-\alpha}]^{\frac{1}{1-\alpha}}. \tag{4}$$

On the other hand, for $0 < \alpha < 1$, the decay rate x^{α} of Eq. (1) remains significant for small x, so much so that all initial values smaller than a threshold value x_t^- will hit zero in a finite time t. More precisely, the interval $x \in [0,x_t^-)$ is mapped by the dynamics into 0 in the finite time t, with

$$x_t^- = [(1 - \alpha)t]^{\frac{1}{1-\alpha}}. \tag{5}$$

This value is obtained by finding the value x_0 for which the denominator of Eq. (2) vanishes, $1 + (\alpha - 1)x_0^{\alpha-1}t = 0$.

We mention in passing that one finds related opposite phenomena, i.e., reaching infinity or escaping zero in a finite time, by considering $y = 1/x$ with $\dot{y} = y^{2-\alpha}$, with the understanding that the solution to such an equation is only unique if the speed $\dot{y}$ has no singularity at the initial point [21].

In the following, we focus on Eq. (1) with $\alpha \geqslant 1$. We will illustrate several results for the particular choice $\alpha = 3$. In this case one has:

$$x_t = \frac{x_0}{\sqrt{1 + 2t x_0^2}}, \quad x_t^+ = \frac{1}{\sqrt{2t}}. \tag{6}$$

These results are valid for all real values of x, with $x \in (-\infty,+\infty)$ mapped by the dynamics into the interval $(-x_t^+,+x_t^+)$.

III. DISTRIBUTED INITIAL CONDITIONS

The dynamics (1) with $\alpha > 1$ maps all the large initial conditions to the neighborhood just below x_t^+. This raises the question as to what happens when the initial probability distribution has a fat tail, i.e., carries a significant probability weight for large x values. Let $P_0(x)$ denote the distribution of the initial conditions x_0. The probability distribution $P_t(x)$ for the resulting x values at time t is obtained from the conservation of probability upon transformation of variables (that is, from x_0 to $x = x_t$):

$$P_t(x_t) = P_0(x_0)\left|\frac{dx_0}{dx_t}\right|. \tag{7}$$

By solving for $x_0(x_t)$ and calculating the derivative $dx_0/dt = (x_0/x_t)^{\alpha}$ from (1), one thus finds:

$$P_t(x) = P_0\left\{x\left[1 - \left(\frac{x}{x_t^+}\right)^{\alpha-1}\right]^{\frac{1}{1-\alpha}}\right\}\left[1 - \left(\frac{x}{x_t^+}\right)^{\alpha-1}\right]^{\frac{\alpha}{1-\alpha}} \tag{8}$$

for $x \in (-x_t^+,+x_t^+)$, and $P_t(x) = 0$ otherwise.

To study the possible accumulation of probability for $P_t(x)$ in the vicinity of x^+, we consider the following fat tail:

$$P_0(x) \sim x^{-\beta}. \tag{9}$$

One finds from Eq. (8) for x smaller than, but close to, x_t^+

$$P_t(x) \sim x^{-\beta}[1 - (x/x_t^+)^{\alpha-1}]^{\frac{\alpha-\beta}{1-\alpha}}. \tag{10}$$

We conclude that the distribution $P_t(x)$ has a divergence for $x \to x_t^+$ for a sufficiently strong fat tail, i.e., when $\beta < \alpha$. The divergence is normalizable since $\beta > 1$ in order for P_0 to be normalizable. For $\beta = \alpha$, $P_t(x)$ converges to a nonzero value for $x \to x_t^+$, while $P_t(x_t^+) = 0$ for $\beta > \alpha$.

As an interesting particular case, we focus on Lorentzian initial conditions,

$$P_0(x) = \frac{\lambda}{\pi}\frac{1}{\lambda^2 + x^2}. \tag{11}$$

One finds from Eq. (8)

$$P_t(x) = \frac{\lambda}{\pi}\frac{[1 + (1 - \alpha)t x^{\alpha-1}]^{\frac{\alpha}{1-\alpha}}}{\lambda^2 + x^2[1 + (1 - \alpha)t x^{\alpha-1}]^{\frac{2}{1-\alpha}}} \tag{12}$$

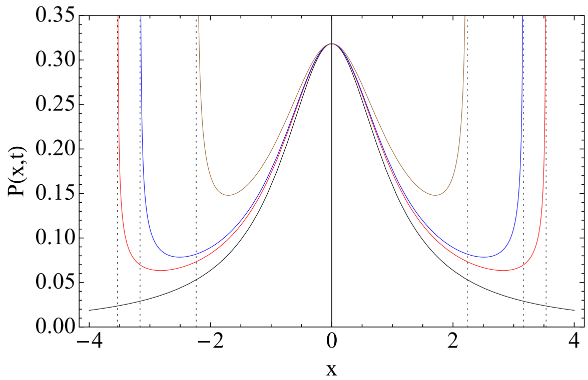

FIG. 1. (Color online) Time evolution of an initial Lorentzian distribution Eq. (11) with $\lambda = 1$ under the deterministic dynamics Eq. (1) with $\alpha = 3, \gamma = 1$ $(t = 0, 0.04, 0.05, 0.10)$. The initial distribution $t = 0$ is shown as a black curve. Time increases from black to brown $(t = 0.10)$. Note the divergences of the probability distribution at the endpoints of the interval $(-1/\sqrt{2t}, 1/\sqrt{2t})$.

for $x \in (-x_t^+, x_t^+)$, and $P_t(x) = 0$ otherwise. In particular, one has for $\alpha = 3$ (see also Fig. 1):

$$P_t(x) = \frac{\lambda}{\pi} \frac{1}{\sqrt{1 - 2tx^2}[x^2 + \lambda^2(1 - 2tx^2)]}, \quad x \in (-1/\sqrt{2t}, 1/\sqrt{2t}). \tag{13}$$

Note the divergences at the endpoint of the interval $[-1/\sqrt{2t}, 1/\sqrt{2t})$. In particular,

$$P_t(x)_{x \to 1/\sqrt{2t}} \sim \frac{\sqrt{2}\, t}{\pi \sqrt{1 - x\sqrt{2t}}}. \tag{14}$$

IV. LINEAR RELAXATION WITH NOISE

Our main purpose is to study the relaxation in the presence of additive noise. No exact analytic results are available for the case of nonlinear relaxation. Hence we first turn to the study of linear relaxation with the exponent $\alpha = 1$. As we show below, this case can be studied in analytic detail, with the additional bonus that it is an interesting and revealing borderline case, in particular with respect to the persistence of the long tails. We consider the following linear Langevin equation:

$$\frac{dx}{dt} = -\gamma x + \xi, \tag{15}$$

with ξ Gaussian white noise with mean value and correlations:

$$\langle \xi(t) \rangle = 0, \tag{16}$$

$$\langle \xi(t)\xi(t') \rangle = 2D\gamma\delta(t - t'). \tag{17}$$

In the following, we again set $\gamma = 1$ by a suitable rescaling of the time variable $t \to \gamma t$ and the noise intensity $D \to D/\gamma$. One could also scale out the noise intensity (i.e., set $D = 1$ by a redefinition of variables provided $D > 0$), but we keep the D dependence in order to reproduce the noiseless limit $D = 0$ discussed in the previous section. The equivalent Fokker-Planck equation reads:

$$\frac{\partial P_t(x)}{\partial t} = \frac{\partial}{\partial x}[x\ P_t(x)] + D\frac{\partial^2}{\partial x^2}P_t(x). \tag{18}$$

The exact solution for the probability distribution $P_t(x)$, starting from a δ-function distribution $P_0(x) = \delta(x - x_0)$, is a Gaussian with first two central moments

$$\mu_t = \langle x \rangle_t = x_0 e^{-t}, \tag{19}$$

$$\sigma_t^2 = \langle (\delta x)^2 \rangle_t = D(1 - e^{-2t}). \tag{20}$$

For a general initial condition $P_0(x)$ one thus finds:

$$P_t(x) = \int dx_0 \frac{e^{\frac{-(x-\mu_t)^2}{2\sigma_t^2}}}{\sigma_t\sqrt{2\pi}} P_0(x_0). \tag{21}$$

We now introduce the Fourier transform, $\hat{P}_t(k) = \int_{-\infty}^{\infty} dx\, e^{ikx} P_t(x)$, which coincides with the moment-generating function:

$$\langle e^{ikx} \rangle_t = \sum_{n=0}^{\infty} \frac{(ik)^n}{n!} \langle x^n \rangle_t, \tag{22}$$

when all moments exist. One finds:

$$\hat{P}_t(k) = e^{-\frac{1}{2}\sigma_t^2 k^2}\, \hat{P}_0(k\ e^{-t}), \tag{23}$$

where $\hat{P}_0(k)$ is the Fourier transform of the initial distribution $P_0(x)$. This result leads to the following general conclusion. Consider an initial distribution with a long tail in the sense that some or all of its moments are divergent. The divergence of moments is equivalent to the fact that the moment-generating function cannot be written as a Taylor expansion around $k = 0$, i.e., it is a nonanalytic function of k at $k = 0$. According to Eq. (23), this nonanalyticity will not be removed and in fact will persist for all time while keeping the same character (same type of nonanalyticity). Nevertheless, the influence of the nonanalyticity is suppressed exponentially in time. We conclude that, while strictly speaking, any type of long tail will persist in the same form for all finite times, its effect will become very difficult to observe for times much longer than the decay time as its weight is exponentially suppressed.

To investigate the situation in more detail, we turn to Lorentzian initial conditions, cf. Eq. (11). From the known result

$$\hat{P}_0(k) = e^{-\lambda|k|}, \tag{24}$$

we get

$$\hat{P}_t(k) = e^{-|k|\lambda_t - \frac{1}{2}\sigma_t^2 k^2}, \tag{25}$$

$$\lambda_t = \lambda e^{-t}. \tag{26}$$

Transforming back to real space, one obtains after a simple manipulation,

$$P_t(x) = \frac{1}{\pi}\int_{-\infty}^{+\infty} dk\ \hat{P}_t(k) = \frac{e^{-\mu_t^2/2\sigma_t^2}}{\pi}\int_{\mu_t/\sigma_t^2}^{\infty} dq\ \cos\left(x\left(q - \frac{\mu_t}{\sigma_t^2}\right)\right)e^{-\frac{1}{2}\sigma_t^2 q^2}. \tag{27}$$

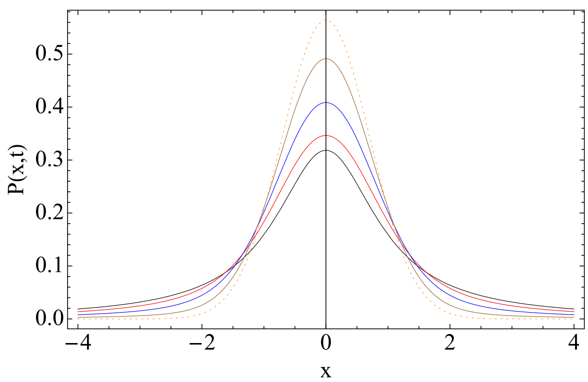

FIG. 2. (Color online) Convergence of the initial Lorentzian distribution to the Gaussian distribution under linear Langevin evolution. The initial distribution is shown as a black curve. Time increases from bottom to top. The dotted curve is the steady-state Gaussian distribution.

Using the tabulated integral

$$\int_0^b dx\, \cos(2ax)e^{-x^2} = \frac{e^{-a^2}}{4}\sqrt{\pi}[\mathrm{erf}(b+ia)+\mathrm{erf}(b-ia)]$$

as well as the property $\mathrm{erf}(\bar{z}) = \overline{\mathrm{erf}(z)}$, Eq. (27) can alternatively be expressed as

$$P_t(x) = \Re\left[\frac{e^{-(x-i\lambda_t)^2/2\sigma_t^2}}{\sigma_t\sqrt{2\pi}}\mathrm{erfc}\left(\frac{ix+\lambda_t}{\sigma_t\sqrt{2}}\right)\right], \tag{28}$$

where $\mathrm{erfc}(z) = 1 - \mathrm{erf}(z)$ is the complementary error function. The time evolution of the probability distribution starting from an initial Lorentzian form to the final Gaussian shape can be observed in Fig. 2.

In the limit of vanishing noise, $D \to 0$, this result reduces to the deterministic limit, cf. limit $\alpha \to 1^-$ of Eq. (12):

$$\lim_{D\to 0} P_t(x) = \frac{1}{\pi}\frac{\lambda_t}{x^2+\lambda_t^2}, \tag{29}$$

where we have used the following asymptotic form of the error function, cf. [22]:

$$\mathrm{erfc}(z)_{|z|\to\infty} \sim \frac{e^{-z^2}}{z\sqrt{\pi}}. \tag{30}$$

This asymptotic form assumes $\arg(z) < 3\pi/4$, a condition satisfied by the argument of the error function in Eq. (28).

Turning to the long-time limit $t \to \infty$, one finds that the distribution function Eq. (28) converges, as expected, to the Gaussian stationary solution of Eq. (30):

$$P^{st}(x) = \frac{e^{-\frac{x^2}{2D}}}{\sqrt{2\pi D}}. \tag{31}$$

However, the approach to this asymptotic result retains, at all finite times, the trace of the initial long-tailed distribution. Indeed, as already indicated via the analysis in Fourier space, cf. Eq. (25), the asymptotic decay of the distribution as $1/x^2$ for $x \to \infty$ persists for all times, even though it is exponentially suppressed in time. This can be derived directly from the explicit expression Eq. (28) for the probability density, by again invoking Eq. (29) (see also Fig. 3):

$$P_t(x)_{|x|\to\infty} \sim \frac{\lambda e^{-t}}{\pi}x^{-2}. \tag{32}$$

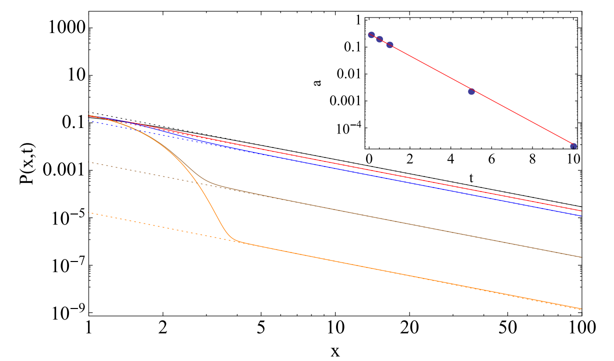

FIG. 3. (Color online) Tails of the distributions shown in Fig. 2 on a log-log plot. Dotted lines represent fits: ax^{-2}. The amplitude a decreases exponentially with time as shown in the inset.

V. NONLINEAR RELAXATION WITH NOISE

We now turn to the investigation of the behavior of long-tailed distributions under nonlinear relaxation with noise,

$$\frac{dx}{dt} = -\gamma x^\alpha + \xi, \tag{33}$$

with equivalent Fokker-Planck equation

$$\frac{\partial P_t(x)}{\partial t} = \frac{\partial}{\partial x}[\gamma x^\alpha\ P_t(x)]\ +\ D\frac{\partial^2}{\partial x^2}P_t(x). \tag{34}$$

We first note that a simple dimensional analysis leads to the general scaling relation

$$P_t(x;D,\gamma) = \left(\frac{\gamma}{D}\right)^{\frac{1}{\alpha+1}} P_\tau(\zeta), \quad \zeta = \left(\frac{\gamma}{D}\right)^{\frac{1}{\alpha+1}} x, \qquad \tau = (\gamma^2 D^{\alpha-1})^{\frac{1}{\alpha+1}} t, \tag{35}$$

which, without loss of generality, allows us to set $\gamma = D = 1$ in the Fokker-Planck equation.

An object of prime interest is the Green's function $G_t(x|x_0)$, i.e., the solution of Eq. (33) for the initial condition $P_0(x) = \delta(x - x_0)$. The general solution of Eq. (33) can then be written as:

$$P_t(x) = \int dx_0 G_t(x|x_0)P_0(x_0). \tag{36}$$

When comparing with the linear case, cf. Eq. (21), two different difficulties are encountered in the application of this result, for example to an initial Lorentzian distribution. First, the explicit expression for $G_t(x|x_0)$ is not known. Second, and in our context more importantly, $G_t(x|x_0)$ does not have the simple dependence on $x - \mathrm{const} \times x_0$, which, in the linear case, allowed us to write the above integral as a convolution. That led to the simple explicit expression Eq. (23) in Fourier space, with the immediate conclusion that initial long tails in the linear case survive for all times. As we will see below, and as expected from the previous deterministic analysis, this is no longer the case for stronger than linear relaxation.

Before turning to a numerical solution of Eq. (34), we present a perturbative solution for the Green's function, revealing a surprising feature about the interplay between nonlinear relaxation and noise. We suppose that the stochastic trajectory x starting at a given initial position x_0 can be well approximated by the deterministic trajectory x_t starting at the same initial position, $x = x_t + \delta x$ with δx small. This approximation is expected to be valid for short times. The explicit form for x_t is given in Eq. (2). The equation for δx reads:

$$\frac{d}{dt}\delta x = -\alpha\, x_t^{\alpha-1}\delta x + \xi, \tag{37}$$

where we neglected terms of order $(\delta x)^2$. This approximation is expected to be valid when $\langle(\delta x)^2\rangle_t \ll x_t^2$. We conclude that δx is a Gaussian random variable, hence we need only evaluate its first two moments. Since the initial condition for the deterministic trajectory is the same as the initial condition of the stochastic trajectory, we have that $\langle\delta x\rangle_{t=0} = 0$ and hence $\langle\delta x\rangle_t = 0$ at all times. For the second moment $\langle(\delta x)^2\rangle_t$, we find:

$$\frac{d\langle(\delta x)^2\rangle_t}{dt} = -2\alpha\, x_t^{\alpha-1}\langle(\delta x)^2\rangle_t + 2 \tag{38}$$

$$= -\frac{2\alpha}{(\alpha-1)t + x_0^{1-\alpha}}\langle(\delta x)^2\rangle_t + 2. \tag{39}$$

We conclude that the short time motion corresponds to the deterministic trajectory, onto which is superimposed a Brownian motion in a harmonic well with spring constant softening as 1/time. This has the following surprising consequence. The Green's function is Gaussian in the short-time limit, but displays two different diffusive regimes. Indeed, one finds from Eq. (38) that

$$\langle(\delta x)^2\rangle_t = 2\int_0^t d\tau \left\{\frac{(\alpha-1)\tau + x_0^{1-\alpha}}{(\alpha-1)t + x_0^{1-\alpha}}\right\}^{\frac{2\alpha}{\alpha-1}}, \tag{40}$$

where we used the fact that $\langle(\delta x)^2\rangle_{t=0} = 0$. At very short times, the ballistic deterministic dynamics ($\sim t$) is slow compared to the diffusion induced by the noise term ($\sim\sqrt{t}$), and we have a usual diffusive regime:

$$\langle(\delta x)^2\rangle_t = 2t \quad \text{for} \quad x_0^{1-\alpha} \gg (\alpha-1)t, \tag{41}$$

cf. the similar expression in the short-time regime for linear relaxation, Eq. (20). In the case of nonlinear relaxation, for instance $\alpha = 3$, the time regime in which this behavior can be observed is very small for $x_0 > 1$. For longer times [but still short enough such that $\langle(\delta x)^2\rangle \ll x_t^2$], one, however, finds a second diffusive regime, but with suppressed diffusion coefficient:

$$\langle(\delta x)^2\rangle_t = \frac{\alpha-1}{3\alpha-1}2t \quad \text{for} \quad x_0^{1-\alpha} \ll (\alpha-1)t. \tag{42}$$

The suppression is by a factor 4 for $\alpha = 3$ and by a factor 7/2 for $\alpha = 5$. Note that the crossover time between the two regimes is given by the condition $x_0 = x_t^+$, that is, the crossover time for a given x_0 is equal to the time needed for the deterministic dynamics to come down to x_0 from infinity, cf. Eq. (3). In particular, the time diverges for the case of linear relaxation $\alpha = 1$, and hence this second diffusive regime ceases to exist in that case.

One can use the short-time Gaussian form for the Green's function to get an approximate solution for distributed initial conditions, namely:

$$P_t(x)_{t\to 0} \approx \int dx_0 \frac{e^{\frac{-(x-x_t)^2}{2\sigma_t^2}}}{\sigma_t\sqrt{2\pi}} P_0(x_0), \tag{43}$$

where x_t is the deterministic trajectory specified in Eq. (2) and $\sigma_t^2 = \langle(\delta x)^2\rangle_t$, as given in Eq. (42). A numerical analysis confirms that this approximation is quite good in this time regime for large x_0 and, therefore, correctly reproduces the short-time behavior of the tail of the distribution. By changing variables $x_0 \to x_t$ we can use the property $P_t^{\text{det}}(x_t)dx_t = P_0(x_0)dx_0$ where $P_t^{\text{det}}(x_t)$ is the deterministic pdf as given in Eq. (8). Hence one can explicitly perform the Fourier transform of Eq. (43):

$$\hat{P}_t(k) = e^{-\frac{\sigma_t^2}{2}k^2}\hat{P}_t^{\text{det}}(kx_t). \tag{44}$$

It is difficult to obtain exact analytic results valid for all times, so we next turn to numerical simulations. These were obtained from the integration of the Fokker-Planck equation using the numerical method described in the Appendix.

First, we confirm the existence of the two different diffusive regimes. We numerically evaluate the Green's function starting from the value $x_0 = 5$ for $\alpha = 3$ and $\alpha = 5$. We clearly identify three time regimes. In the first two time regimes, the Green's function is Gaussian, but displays the above predicted switch over from a $\langle(\delta x)^2\rangle_t \sim 2t$ to a $\langle(\delta x)^2\rangle_t \sim \frac{\alpha-1}{3\alpha-1}2t$ behavior. This is illustrated in more detail in Fig. 4, where we plot $\langle(\delta x)^2\rangle_t$ as a function of time. The third time regime corresponds to the relaxation to the steady state, with a saturation value

$$\frac{\int_{-\infty}^{\infty} dx\, x^2 e^{-x^{\alpha+1}/\alpha+1}}{\int_{-\infty}^{\infty} dx\, e^{-x^{\alpha+1}/\alpha+1}} = 0.675978\ldots, \quad \alpha = 3$$

$$= 0.578617\ldots, \quad \alpha = 5. \tag{45}$$

Second, in Fig. 5 we reproduce the relaxation of an initial Lorentzian distribution in a potential with $\alpha = 3$. Again, the numerical results are in full agreement with the analysis given above. We recall that the deterministic relaxation projects the entire real axis onto a finite interval $(-x_t^+, x_t^+)$, with normalizable divergences at the boundaries. The effect of the additive noise is to wash out the divergences, leading to Gaussian peaks in the vicinity of $\pm x_t^+$, with diffusive spreading described by Eq. (42), $\langle(\delta x)^2\rangle_t \sim t/2$. Both peaks move in towards zero relatively slowly, as $1/\sqrt{t}$. This picture is valid for short to intermediate times. Note also the somewhat surprising nonmonotonic behavior in time of the probability density in the vicinity of $x = 0$. Probability mass first flows out of this region, with the density decreasing below the Lorentzian values. At a later time, the probability peaks generated by the deterministic dynamics from the tails of the initial distribution bring in probability mass towards the center region, and the probability density again increases to finally attain its steady-state value, which is above the Lorentzian value. The appearance of the additional peaks is however not a feature unique to the Lorentzian initial state. It can happen for other appropriate initial distributions. They have to be such that the initial peak

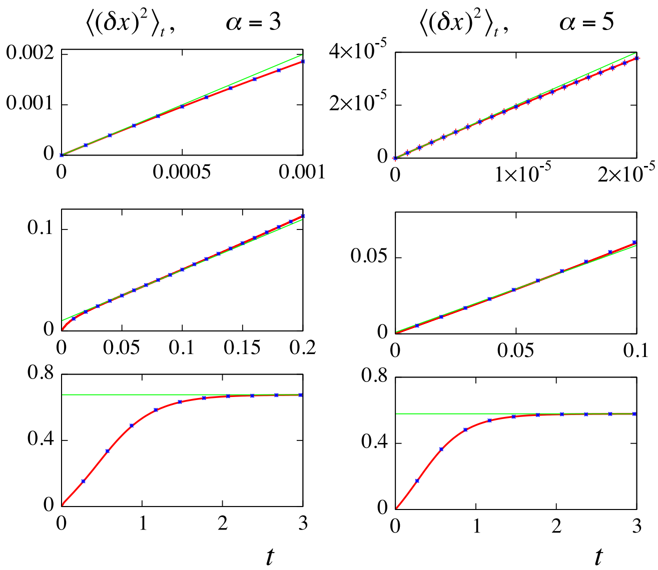

FIG. 4. (Color online) Plot of the time dependence of the variance $\langle(\delta x)^2\rangle_t$ of the probability distribution $P_t(x)$.The numerical results of the integration of the Fokker-Planck equation Eq. (34) are given by the red curves, while the dots denote the results of a direct numerical integration of the Langevin equation using the stochastic Heun method. Left column: $\alpha = 3$; right column: $\alpha = 5$. The initial condition is a δ function centered at $x_0 = 5$. We clearly see the three regimes predicted by the theory. Top: early time with normal diffusion where the variance $\langle(\delta x)^2\rangle_t$ grows as $2t$ indicated by green lines, cf. Eq. (41). Middle: intermediate time with a reduced diffusion, the variance growing as $t/2$ for $\alpha = 3$ and as $4t/7$ for $\alpha = 5$, indicated by green lines, cf. Eq. (42). Bottom: late-time saturation where the asymptotic values, indicated by green lines, are given by Eq. (45).

value is below the steady-state value, while the corresponding initial peak steepness is larger than that of the steady state. The latter condition ensures that probability will initially flatten with probability leaving the peak region, while the former one implies that probability mass ultimately has to return to the peak to restore the steady-state value. Both conditions are met for the initial Lorentzian distribution.

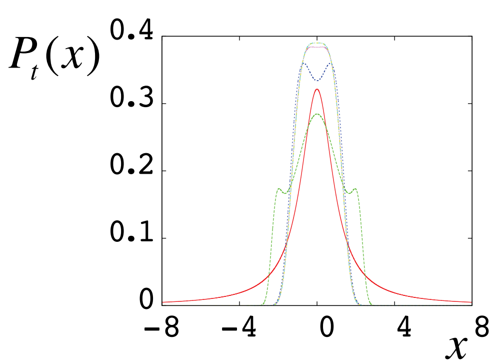

FIG. 5. (Color online) Probability distribution functions obtained from a numerical integration of the Fokker-Planck equation, Eq. (34), for $\alpha = 3$ and $\gamma = 1$, $D = 1$ using the method explained in the Appendix. The initial condition is the Lorentzian distribution Eq. (11) with $\lambda = 1$. From red to purple (outwards to inwards) the curves correspond to $t = 0, 0.01, 0.1, 0.5, 1, 10$, the last curve coinciding exactly with the stationary distribution $P_{st}(x) = \frac{\sqrt{2}}{\Gamma(1/4)} e^{-x^4/4}$.

VI. DISCUSSION

A large number of phenomena in science are described in terms of linear dynamics. Yet, linear relaxation, $\dot{x} = -x$ and the concomitant exponential dependence on time, $\exp(-t)$, describe borderline situations when compared to nonlinear dynamics $\dot{x} = -x^\alpha$, with $\alpha \neq 1$. For example, if an initial condition includes contributions at $x \to \infty$, the exponential takes an infinitely long time to bring these contributions down from infinity. Any initial condition takes forever to reach $x = 0$. In other words, any initial contribution that decreases with time takes an infinite time to reach the final condition. This is no longer the case when nonlinear relaxation is considered. Trajectories come down from infinity instantaneously for an exponent $\alpha > 1$, while trajectories corresponding to an exponent $\alpha < 1$ hit zero in a finite time.

In this paper, we showed that linear dynamics remains a borderline case in the presence of additive noise ($\dot{x} = -x^\alpha + \xi$ with ξ Gaussian white noise). We focused on the comparison between linear relaxation $\alpha = 1$ and nonlinear relaxation with $\alpha > 1$. We found that linear dynamics will sustain long tails for all times, if initially present, even though the weight of these tails is suppressed exponentially in time. Nonlinear relaxation, however, will instantaneously kill any long tails. As an unexpected byproduct of our analysis, we mention the discovery of a second diffusive regime for noisy nonlinear dynamics. By this we mean the following. The propagator (Green's function) for the linear Langevin equation is exactly Gaussian. The average follows the exponential decay dictated by the deterministic dynamics. The variance σ^2 displays the expected short-time diffusive behavior $\sigma^2 = 2Dt$, where D is the noise intensity, followed by saturation towards the steady value for larger times. For nonlinear dynamics with additive noise, the propagator is still Gaussian in a short-time regime. The average again reproduces the (nonlinear) deterministic dynamics. The variance has an interesting behavior different from that of the linear problem. Apart from the usual short-time behavior $\sigma^2 = 2Dt$, which the nonlinear problem also exhibits, another regime of linear dispersion follows as time increases, but with reduced coefficient, i.e., $\sigma^2 = 2D't$ with $D' = D(\alpha - 1)/(3\alpha - 1)$. This second regime of suppressed diffusion is actually the dominant regime before the saturation to the steady state, for initial conditions starting sufficiently far away from zero. The crossover time between the two regimes scales as $x_0^{1-\alpha}/(1-\alpha)$, which diverges as $\alpha \to 1$. Therefore, notably, the second regime is completely absent for linear dynamics.

ACKNOWLEDGMENTS

R.T. and C.V.d.B. acknowledge the warm hospitality at UCSD where this work was carried out. U.H. acknowledges the support of the Indian Institute of Science, India. R.T. acknowledge financial support from EU (FEDER) and the Spanish MINECO under Grant INTENSE@COSYP (FIS2012-30634) and C.V.d.B. from MO 1209 COST action of the European Community. K.L. gratefully acknowledges support by the U.S. Office of Naval Research (ONR) under Grant No. N00014-13-1-0205.

APPENDIX: NUMERICAL INTEGRATION OF EQ. (34)

For the numerical integration of Eq. (34) we have used a splitting method [23] combining the exact solutions of the purely deterministic ($D = 0$) and purely stochastic ($\gamma = 0$) limits of the equation. They read respectively [we use the notation $P(x,t)$ for $P_t(x)$]

$$P(x,t+h) = [1 + (1-\alpha)\gamma h x^{\alpha-1}]^{\frac{\alpha}{1-\alpha}} \times P\{x[1 + (1-\alpha)\gamma h x^{\alpha-1}]^{\frac{1}{1-\alpha}},t\}, \quad \text{(A1)}$$

$$\hat{P}(k,t+h) = e^{-Dhk^2}\hat{P}(k,t), \quad \text{(A2)}$$

where we use the expression in Fourier space for the stochastic solution. In the numerical method we discretize space $x_i = i dx$, $i \in [-M+1,M]$. Hence, $P_i(t)$ accounts for the probability in the whole interval $[x_i,x_{i+1})$. After setting the initial condition $P_i(t=0)$, the method works as follows:

(i) Given x_i, $i \in [-M+1,M]$, compute $x_i' = x_i(1 + (1-\alpha)\gamma h x_i^{\alpha-1})^{\frac{1}{1-\alpha}} \equiv a_i x_i$. Find the index $i' = \text{floor}[x_i'/dx]$. [The function floor$[z]$ is defined as the largest integer less than or equal to the real (positive or negative) number z]. Implement Eq. (A1) using linear interpolation in the interval $[x_{i'},x_{i'+1})$, namely:

$$P_i'(t) = a_i^{\alpha}\{[P_{i'+1}(t) - P_{i'}(t)]\cdot(ia_i - i') + P_{i'}(t)\}. \quad \text{(A3)}$$

(ii) Compute the Fourier transform $\hat{P}_q'(t)$ of $P_i'(t)$ with $q \in [-M+1,M]$. Apply Eq. (A2) using

$$\hat{P}_q(t+h) = e^{-Dhk_q^2}\hat{P}'_q(t), \quad k_q = \frac{\pi}{M dx}q. \quad \text{(A4)}$$

Invert the Fourier transform to find $P_i(t+h)$.

Although this method is accurate only to order $O(h)$, we have found it more convenient than the use of a finite difference expression for the partial derivatives and then a higher-order precision integration method, such as second-order Runge-Kutta. It is known that the von Neumann stability analysis leads to the Courant-Friedrichs-Lewy criterion that determines that the time step h should vary as the square of the spatial discretization step, $(dx)^2$, and therefore this method requires very small time steps and large integration times [24]. The splitting method we use, on the other hand, is able to handle the stiffness of the deterministic part as well as implementing a very efficient pseudospectral algorithm for the stochastic part.

For the calculations of the Fourier transforms we have used fast Fourier routines. We typically take $M = 2^{16}$ and $dx = 10^{-3}$, so the interval value for x is approximately $(-65.5,+65.5)$. Depending on initial conditions we use $h = 10^{-3}, 10^{-4}, 10^{-5}$ and check in every case that results with smaller values of h do not deviate significantly.

[1] J. Klafter, S. C. Lim, and R. Metzler, *Fractional Dynamics, Recent Advances* (World Scientific, Singapore, 2012); R. Metzler, G. Oshanin, and S. Redner, *First-passage Phenomena and Their Applications* (World Scientific, Singapore, 2014); V. Méndez, D. Campos, and F. Bartumeus, *Stochastic Foundations in Movement Ecology* (Springer, Berlin, 2014).

[2] N. G. Van Kampen, *Stochastic Processes in Physics and Chemistry* (North Holland, Amsterdam, 1992).

[3] F. Marchesoni, Prog. Theor. Phys. **74**, 1339 (1985).

[4] N. Pomphrey, J. D. Meiss, and K. M. Watson, J. Geophys. Res. **85**, 1085 (1980).

[5] Yu. P. Kalmykov, NATO Science Series II: Mathematics, Physics and Chemistry **157**, 31 (2005).

[6] R. Zhang and K. S. Schweizer, J. Chem. Phys. **136**, 154902 (2012).

[7] W. Alexiewicz and K. Grygiel, Acta Phys. Pol. A **114**, 687 (2008).

[8] W. T. Coffey, Yu. P. Kalmykov, and E. S. Massawe, Phys. Rev. E **48**, 77 (1993).

[9] B. Lindner, J. Stat. Phys. **130**, 523 (2008).

[10] I. M. Sokolov, Europhys. Lett. **44**, 278 (1998).

[11] C. Van den Broeck, M. Malek Mansour, and F. Baras, J. Stat. Phys. **28**, 557 (1982); F. Baras, M. Malek Mansour, and C. Van den Broeck, *ibid.* **28**, 577 (1982).

[12] C. Van den Broeck and P. Mandel, Phys. Lett. A **122**, 36 (1987).

[13] D. K. Kondepudi and G. W. Nelson, Nature (London) **314**, 438 (1985).

[14] P. Gaspard and X. Wang, Proc. Natl. Acad. Sci. USA **85**, 4591 (1988); N. Korabel and E. Barkai, Phys. Rev. Lett. **102**, 050601 (2009).

[15] There is a large literature on this subject. We only cite one of the early papers: D. Sigeti and W. Horsthemke, J. Stat. Phys. **54**, 1217 (1989).

[16] O. Hirschberg, D. Mukamel, and G. M. Schütz, Phys. Rev. E **84**, 041111 (2011); J. Stat. Mech. (2012) P02001.

[17] See, e.g., *Noise in Nonlinear Dynamical Systems*, Vols. 1–3, edited by F. Moss and P. V. E. McClintock (Cambridge University Press, Cambridge, 1989).

[18] *Nonlinear Dielectric Phenomena in Complex Liquids*, edited by S. J. Rzoska and V. P. Zhelezny (Springer, Berlin, 2005).

[19] P. Reimann, Phys. Rep. **361**, 57 (2002).

[20] P. Hänggi, Rev. Mod. Phys. **62**, 251 (1990).

[21] S. H. Strogatz, *Nonlinear Dynamics and Chaos: With Applications to Physics, Biology, Chemistry and Engineering* (Westview Press, Boulder, 1994).

[22] M. Abramowitz and I. A. Stegun, *Handbook of mathematical functions* (Dover, Mineola, 1965), formula (7.1.23).

[23] H. Holden, K. H. Karlsen, K.-A. Lie, and N. H. Risebro, *Splitting Methods for Partial Differential Equations with Rough Solutions*, EMS Series of Lectures in Mathematics (European Mathematical Society Publishing House Seminar for Applied Mathematics, Zurich, 2010).

[24] R. Toral and P. Colet, *Stochastic Numerical Methods* (Wiley-VCH, New York, 2014).